Supporting Information

Liu et al. 10.1073/pnas.1011845108

SI Materials and Methods

Mice. All animals were housed in a pathogen-free facility at McGill University and were given a standard rodent diet and water ad libitum.

Cell Culture. To determine the effect of the conditioned media on cell growth, TM15 cells (5,000 cells per well in a 12-well plate) were grown in conditioned media obtained from retinoic acid receptor β (*Rarb*)-null or wild-type mouse mammary gland fibroblasts. Cells from three wells per time point were counted on days 2, 4, 6, and 8 after plating. Cell proliferation was measured by ^{3}H-thymidine incorporation assay. One μCi ^{3}H-thymidine was added to each well for the last 4 h of culture after TM15 cells were grown in the conditioned media for 5 d. The cells then were deposited onto harvester filters using a semiautomatic cell harvester. Radioactivity was measured in a scintillation counter, and results were expressed as cpm for individual samples. Each experiment was repeated three times. Mouse mammary fibroblasts were generated as followed: Mammary fat pads from gland no. 4 were cleared to remove epithelial cells as described (1). The gland-free mammary fat pads were put in a 10-mm dish, sprayed with ethanol, and left for 2 min. Then the tissues were washed by PBS and cut into small pieces. The small tissue pieces were placed in six-well plates and allowed to dry. Then 3 mL of culture medium was added and incubated for a few days (medium was changed from time to time). The cells were trypsinized and transferred into a T25 flask (Greiner Bio-One) where they spread and grew to subconfluency. Both *Rarb*$^{-/-}$ and wild-type cells were validated by Western blot with fibroblast- and epithelium-specific antibodies. Finally, the cells were immortalized by being transfected with SV40 to become stable cell lines.

Mammary Whole Mounting and H&E Staining. Whole mounts were prepared following protocols described on the Biology of the Mammary Gland website (http://mammary.nih.gov). All histological slides were scanned into the Aperio Image System and were analyzed by Spectrum Software (Aperio Technologies).

Immunohistochemical Analysis. The following dilutions of primary antibodies were used: rabbit polyclonal anti–human-RARβ (Abcam), 1:100; mouse monoclonal anti-human Ki67 (clone B56; BD Pharmingen), 1:100; rabbit polyclonal anti–human-STAT1 (Upstate), 1:50; rabbit polyclonal anti–human-caspase-3 (Cell Signaling), 1:50; rat monoclonal anti–mouse-CD31 (clone Mec13.3; Biocare), 1:50; mouse monoclonal anti-CD45, 1:100, and rabbit polyclonal anti-mouse collagen I, 1:100 (Abcam Inc.). For the negative control, primary antibody was replaced with nonimmunized rabbit or mouse IgG (Vector Laboratories). All images were taken with 10× objectives (100× magnification). For multiple antigen labeling the VECTASTAIN System (Vector ABCDAB kit, Vector ABC-AP kit, and Vector ImmPRESS NovaRED and VIP kit) (Vector Laboratories) was used. Peroxidase and alkaline phosphatase substrates were used to develop color of the antigens with different localization. The following dilutions of primary antibodies were used: (*i*) rabbit polyclonal anti–human-RARβ (Abcam), 1:50; (*ii*) goat polyclonal anti–human-Vimentin (Abcam), 1:50; (*iii*) horse polyclonal anti-human smooth muscle actin-α (α-SMA) (Abcam), 1:100. To compare positive cell numbers, 10 random fields per section were documented in the Aperio Image System and were analyzed by Spectrum Software. The percentage of positive tumor cell nuclei relative to the total number of cancer cell nuclei was calculated by Spectrum. Mean values shown beside the corresponding images were determined from results from at least six different mice for each genotype.

Western Blotting. Lysates were prepared from the mammary tumors of three *Rarb*$^{-/-}$ and three wild-type mice. Antibodies against phospho-ErbB2/neu (Tyr1248), ErbB2/neu, phospho-Src (Tyr416), Src, phosphor-Akt, and Akt were purchased from Cell Signaling Technology. Antibodies against RARβ (C-19), stromal cell-derived factor 1 (SDF-1) (FL-93), and actin (I-19) were purchased from Santa Cruz Biotechnology. PhosphoPlus Stat1 (Tyr701) Antibody Kit (Cell Signaling Technology) was used according to the manufacturer's instructions.

Apoptosis Analysis. The number of TUNEL-positive or caspase 3-postive tumor cell nuclei was calculated relative to the total number of 1,000 cancer cell nuclei, which was analyzed with the Spectrum software system (Aperio Technologies). Mean values were determined from results from at least six different mice.

Transplantation Studies. Tumor size was determined weekly using caliper measurements in two perpendicular dimensions (length and width). Tumors were collected 8 wk after tumor initiation and were divided into two fragments, one snap frozen and another fixed in 10% neutral-buffered formalin and embedded in paraffin.

Flow Cytometry. Single-cell suspensions of mammary glands for flow cytometry were prepared as described (2) with minor modifications. Specifically, 0.1 mg/mL liberase TL (Roche) and 0.05% DNase I were added, and the tissue was incubated for 60 min at 37 °C with gentle shaking and was filtered through a 70-μm strainer. After cells from different tissues (spleen, thymus, bone marrow, lymph nodes, and mammary glands) were isolated, the cells were surface stained with appropriate dilutions of antibodies determined from titration experiments for 20 min in the dark at 4 °C, fixed in PBS containing 1% formaldehyde, and stored at 4 °C in the dark until FACS analysis (performed within 24 h). The following anti-mouse monoclonal antibodies were used: FITC anti-CD4 (RM4-5), phycoerythrin (PE) anti-CD8/ (53-6.7), PE anti-CD73 (TY/23), PECy7 anti-CD19 (1D3), adenomatous polyposis coli (APC) anti-CD11c (HL3), APC anti-NK1.1 (PK136), and APCCy7 anti-GR1 (RB6-8C5) (all from BD Pharmingen); FITC anti-F4/80 (BM8), PECy5 anti-CD69 (^{1}H.2F3), PECy5 anti-MHC-II (M5/114.15.2), PerCPCy5.5 anti-CD3ε (145-2C11), PE-Cy7 anti-CD45 (30-F11), and eFluor 450 anti-CD105 (MJ7/18) (all from eBioscience). Data were acquired on a LSRII benchtop flow cytometer (BD Biosciences) equipped for the detection of eight fluorescent parameters. A minimum of 1×10^{5} total cells were collected by FACS for each tissue sample. Data analysis was performed using FACS DiVa version 6.0 software. Initial gating of each sample set used a forward scatter (FSC)-area versus an FSC-height plot to gate out cell aggregates. Analysis of mesenchymal stem cells (MSCs) directly from bone marrow involved exclusion of CD3^{+}, CD4^{+}, CD11c^{+}, CD19^{+}, CD45^{+}, NK1.1^{+}, F4/80^{+}, and GR1^{+} hematopoietic lineages, and the remaining events were subjected to a CD73 versus CD105 gate to isolate MSCs.

RNA Isolation. Total RNA was isolated using TRIzol reagent (Invitrogen) according to the manufacturer's instructions, followed by DNase treatment and RNA clean-up (RNeasy mini kit; Qiagen). RNA integrity was determined using the RNA 6000 Nano LabChip Kit on an Agilent 2100 Bioanalyzer (Agilent Technologies).

1. Deome KB, Faulkin LJ. Jr. Bern HA, Blair PB (1959) Development of mammary tumors from hyperplastic alveolar nodules transplanted into gland-free mammary fat pads of female C3H mice. *Cancer Res* 19:515–520.

2. Diehn M, et al. (2009) Association of reactive oxygen species levels and radioresistance in cancer stem cells. *Nature* 458:780–783.

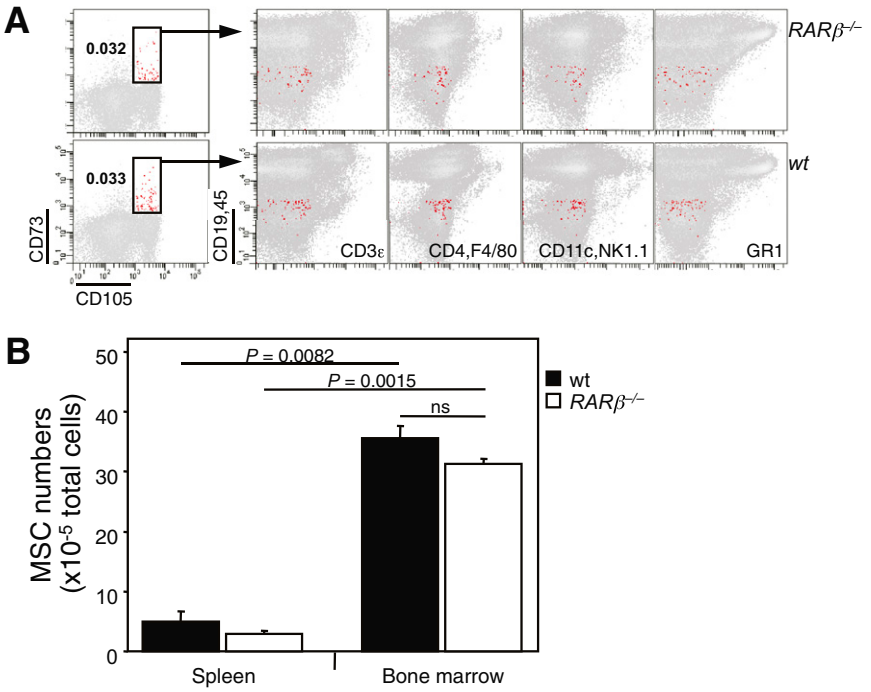

Fig. S1. MSC numbers in bone marrow of *Rarb*$^{-/-}$ versus wild-type mice. (*A*) Immunophenotype of CD73^{+}CD105^{+} MSCs from bone marrow of *Rarb*$^{-/-}$ and wild-type mice. (*B*) Number (mean ± SD) of MSCs from 105 splenocytes and bone marrow cells (one tibia and femur) from 3-mo-old wild-type and *Rarb*$^{-/-}$ mice.

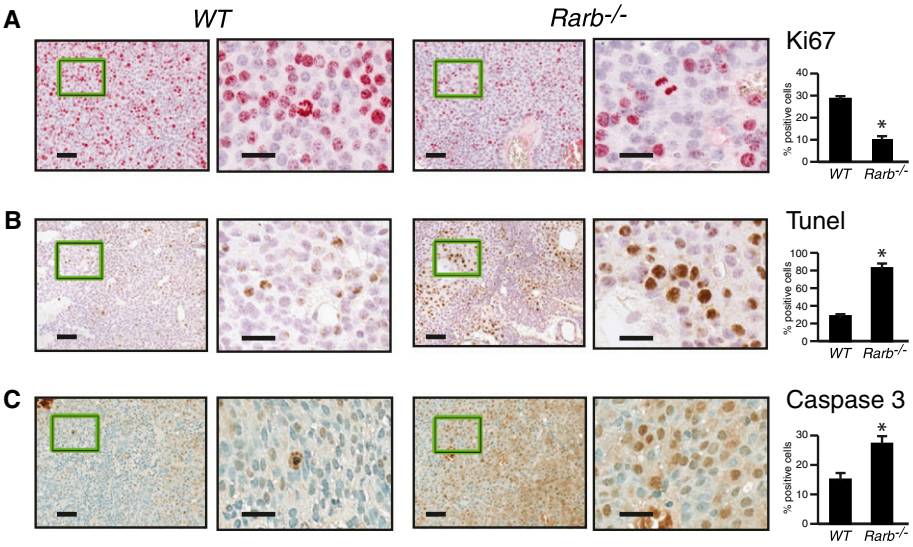

Fig. S2. Loss of *Rarb* affects the growth of mammary tumor cells. (*A*) The cell proliferation rate was identified by Ki67 expression (red signal), which is significantly lower in the tumors from *Rarb*-null mice ($P < 0.001$). (*B*) TUNEL analysis showed significantly increased apoptotic cells in *Rarb*-null mice ($P < 0.001$). (*C*) Caspase 3 is significantly increased in tumor cells from *Rarb* null-animals ($P < 0.01$). [Scale bars: 50 μm for low-magnification images (*Left*) and 20 μm for high-magnification images (*Right*).]

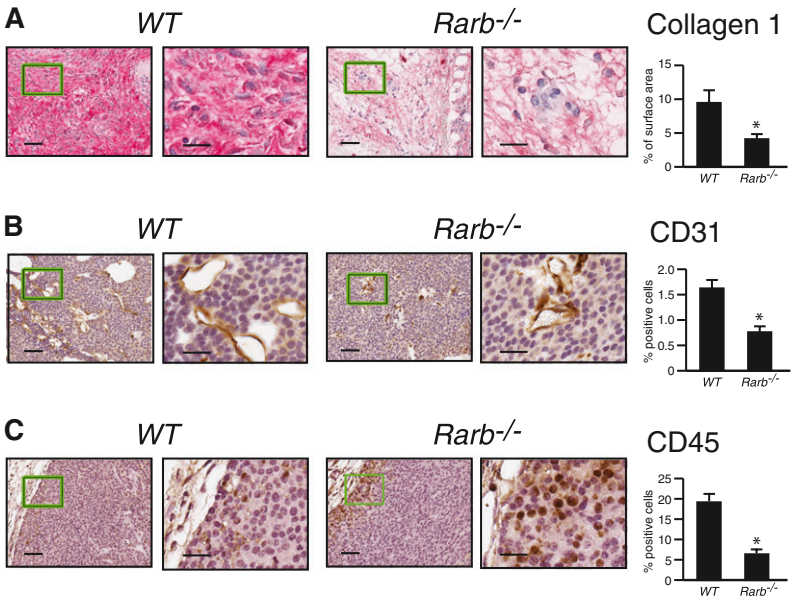

Fig. S3. Inactivation of *Rarb* leads to the remodeling of the tumor microenvironment. (*A*) Paraffin-embedded mammary tumor sections stained for collagen I show a decrease in matrix stiffness and indicate reduced activity of the cancer-associated fibroblasts in the *Rarb*-null tumor microenvironment. Quantification of positive cells is shown at the right. (*B*) Paraffin-embedded mammary tumor sections stained for CD31 demonstrate a reduction of angiogenesis in the *Rarb*-null tumor microenvironment. Quantification of positive cells is shown at the right. (*C*) Paraffin-embedded mammary tumor sections stained for CD45 demonstrate a decreased infiltration of inflammatory cells in the *Rarb*-null stroma. Quantification of positive cells is shown at the right. [Scale bars: 50 μm for low-magnification images (*Left*); 20 μm for high-magnification images (*Right*).]

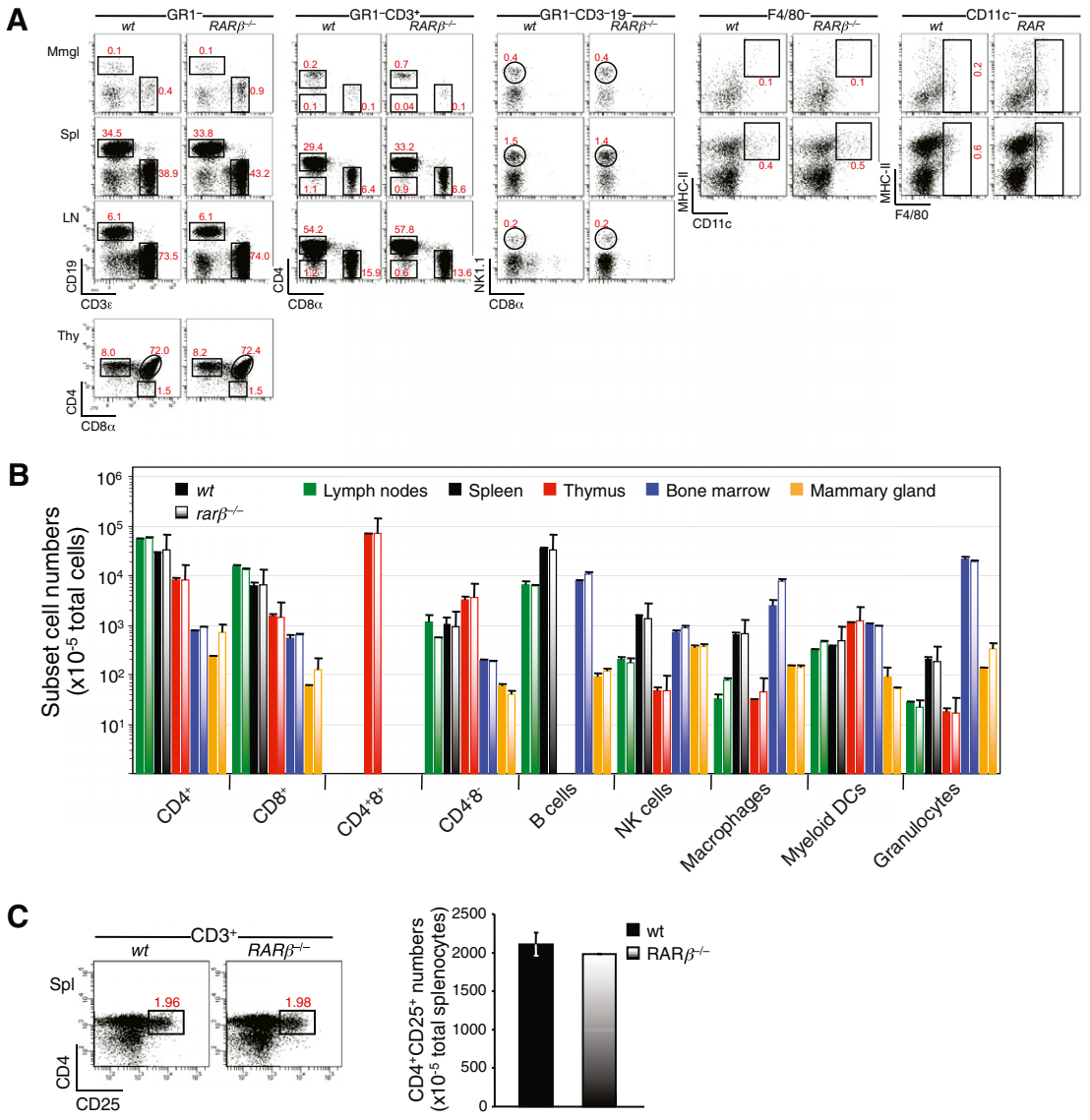

Fig. S4. Normal immune compartments in mouse mammary tumor virus (*MMTV*)-*ErbB2*/*Rarb*$^{-/-}$ versus *MMTV-ErbB2* mice. (*A*) The percentage (in red) of immune cell lineage subsets from the total tissue cellularity was quantified by FACS in the spleen (Spl), thymus (Thy), lymph nodes (LN), mammary gland (Mmgl), and bone marrow (not shown). (*B*) Flow cytometric analysis of immune cell lineage composition expressed as the number (mean ± SD; $n = 2$) of CD4 and CD8 single-positive, CD4$^+$CD8$^+$, and CD4$^-$CD8$^-$ T cells, B cells (CD19$^+$), NK cells (NK1.1$^+$), dendritic cells (CD11c$^+$), macrophages (F4/80$^+$), and granulocytes (GR1$^+$) out of 105 cells from the lymph nodes (popliteal and axial), spleen, thymus, bone marrow (one tibia and femur), or mammary glands of 2-mo-old wild-type and *RARb*$^{-/-}$ mice. (*C*) (*Left*) FACS analysis and (*Right*) quantification (mean ± SD; $n = 2$ mice per genotype) of CD4$^+$CD25$^+$ cells out of 10^5 splenocytes from 3-mo-old wild-type and RARβ$^{-/-}$ mice.

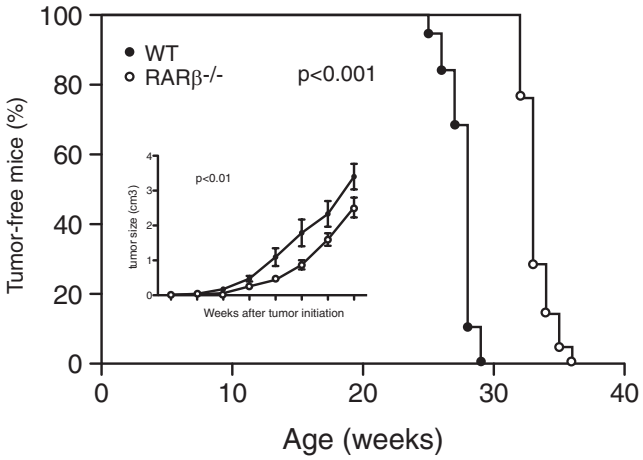

Fig. S5. Donor mice for transplantation experiments confirm that ablation of *Rarb* results in a delay in tumor formation. Wild-type and $Rarb^{-/-}$ mice expressing ErbB2 driven by the MMTV-LTR promoter and used as donor mice for the transplantation experiments (gland no. 4) shown in Fig. 4 of the main text were monitored for tumor formation. T_{50} was 27.66 and 33.11 wk for $Rarb^{-/-}$ (n = 21) and wild-type mice (n = 19), respectively. (*Inset*) The growth rate of the tumors in the $Rarb^{-/-}$ genetic background was delayed significantly ($P < 0.005$; two-way ANOVA) compared with the growth rate of tumors on the wild-type genetic background.

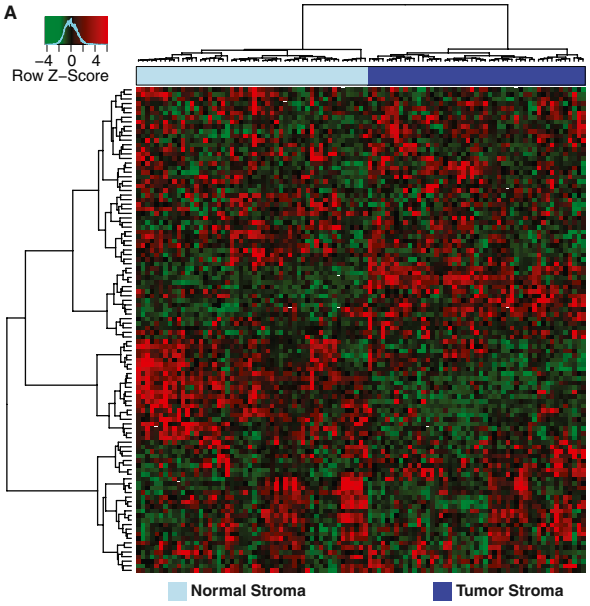

B

Statistical Test	p-value
Wilcoxon test Enrichment of univariate predictors	0.03928
GlobalTest Association of the gene set with tissue type	0.00000

Fig. S6. The RARβ gene set separates tumor from normal stroma. (*A*) Hierarchical clustering and heatmap of the 106 human ortholog RARβ gene set in microdissected normal and tumor stroma samples. (*B*) Statistical tests performed to validate the split between normal and tumor stroma show that the RARβ gene list contains a significant number of genes whose individual expression levels differentiate between tumor and normal stroma (Wilcoxon test; P = 0.03928). A multivariate test that measures how well the gene set jointly differentiates between tumor and normal stroma (GlobalTest, R package, version 4.12.0) was applied also ($P < 10^{-5}$).

Other Supporting Information Files

Table S1 (XLS)
Table S2 (PDF)